Subspace-based System Identification for Helicopter Dynamic Modelling

Ping Li, Ian Postlethwaite and Matthew Turner
Department of Engineering, University of Leicester
Leicester, UK
pl62@leicester.ac.uk, ixp@leicester.ac.uk, mct6@leicester.ac.uk

Abstract

This paper investigates the problem of helicopter dynamic modelling using time-domain system identification techniques. The paper begins with a brief introduction to the state-space form of the perturbation model for helicopters, based on which, system identification modelling is performed. Then the MOESP (Multivariable Output-Error State sPace) subspace identification method is described. Computer simulations are carried out to illustrate the operation and performance of the method using concatenated data sets. The method is then applied to real data from EH101 helicopter flight tests and some preliminary results of identifying an extended dynamic model about the cruise condition are presented.

Introduction

A prerequisite for the design of a satisfactory helicopter flight control system is an appropriate model capable of capturing the main characteristics of the helicopter dynamic behaviour. Fig. 1 shows the block schematic representation of the helicopter flight control loop configuration. The helicopter flight dynamics to be modelled in physical component terms includes the fuselage dynamics, rotor dynamics and engine and transmission system dynamics.

System identification is a modelling method where the model of the system under consideration is obtained from input/output measurement data. The identification can be performed either in the time-domain or in the frequency-domain, but most results of system identification for helicopter applications that have been reported in the literature use frequency-domain methods (see e.g. [1] [2] [3]). Though well-suited for single-input single-output (SISO) model identification, the use of the frequency-domain identification method with time-domain data for multiple-input multiple-output (MIMO) state-space model identification is cumbersome. This is particularly so when multiple inputs are present in the excitation, as in most helicopter flight tests; because, in addition to the conversion of time-domain measurement data to frequency-domain data, a considerable amount of data conditioning is required to remove the contaminating effects of partially-correlated control inputs from the extracted frequency responses. For this reason, this paper will focus on the development and application of time-domain methods for state-space helicopter dynamic modeling via exploitation of recent innovations in system identification techniques. The rest of the paper is organized as follows. Next section briefly introduces the state-space perturbation model for helicopters, based on which the system identification is performed. Then the subspace-based system identification strategy used in this paper is described, which is followed by the simulation studies. The results of helicopter dynamic modelling via subspace-based system identification using real flight test data are presented with concluding remarks in the last section.

[0]To be presented at the American Helicopter Society 63rd Annual Forum,Virginia Beach,VA, May 1-3, 2007.

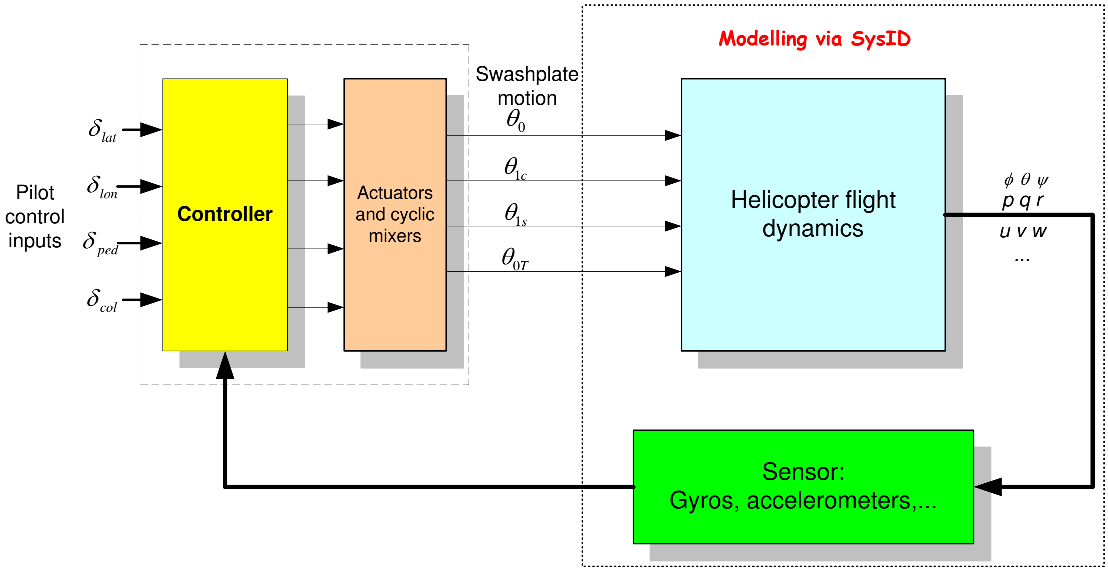

Figure 1: Schematic representation of a helicopter flight control loop configuration

Modelling helicopter flight dynamics

Unlike fixed-wing aircraft, the dynamic behaviour of a helicopter is very complex with strong inter-axis and fuselage-rotor coupling as well as inherent nonlinearities. Therefore, the overall dynamic behaviour of a helicopter is best described by a nonlinear MIMO state-space model. The basic equations of motion for a model of helicopter dynamics are developed from the application of Newton's laws of motion to the fuselage that is free to rotate and translate simultaneously in all six degrees of freedom (DoF). This model can then be extended to include appropriate rotor and other dynamics, for example, for high-bandwidth controller design or for accurate handling quality evaluations where it is essential to account for the dynamic coupling between the rotor and the fuselage. In general, a helicopter dynamic model is of the following nonlinear form [4]:

$$\dot{\mathbf{x}} = \mathbf{F}(\mathbf{x}, \mathbf{u}, t) \tag{1}$$

where $\mathbf{x}$ is the state vector that is composed of the fuselage states such as the translational and rotational velocities, the Euler angles defining the orientation of the fuselage axes relative to the earth, the rotor states such as rotor flapping angles etc. $\mathbf{u}$ is the control input and $\mathbf{F}$ is a vector-valued nonlinear function of the states and control inputs. To develop rational explanations for the dynamic behaviour of a helicopter and to facilitate the helicopter flight control system design, it is often necessary to use a simplified model that is able to capture the main characteristics of the helicopter dynamic behaviour whilst being mathematically tractable. This is achieved by linearizing equation (1) with small perturbation theory, where it is assumed that, during disturbed motion, the helicopter behaviour can be described as a perturbation from the trim condition, written in the form:

$$\mathbf{x} = \mathbf{x}_e + \delta\mathbf{x} \quad \text{and} \quad \mathbf{u} = \mathbf{u}_e + \delta\mathbf{u}$$

where $\mathbf{x}_e$ is the trim state vector and $\mathbf{u}_e$ is the control vector required to maintain the trim condition. The trim condition can, in principle, be obtained by letting the rate of change of the state vector (i.e the left hand side of equation (1)) be identically zero.

A fundamental assumption of linearization is that the function $\mathbf{F}$ in (1) can be represented as a vector valued analytic function of the disturbed state variables, control inputs and their derivatives;

linearization then amounts to neglecting all except the linear terms in the Taylor series expansions of this function about the known trim point $(\mathbf{x}_e, \mathbf{u}_e)$. The linearized model describing perturbed motion of a helicopter about a general trim condition, can then be written as

$$\delta\dot{\mathbf{x}} - \mathbf{A}\delta\mathbf{x} = \mathbf{B}\delta\mathbf{u} \tag{2}$$

where the system (or stability) and control matrices $\mathbf{A}$ and $\mathbf{B}$ in (2) are derived from the partial derivatives of the nonlinear function $\mathbf{F}$, i.e.(see e.g. [4])

$$\mathbf{A} = \left[\frac{\partial \mathbf{F}}{\partial \mathbf{x}}\right]_{\substack{\mathbf{x}=\mathbf{x}_e \\ \mathbf{u}=\mathbf{u}_e}} \tag{3}$$

and

$$\mathbf{B} = \left[\frac{\partial \mathbf{F}}{\partial \mathbf{u}}\right]_{\substack{\mathbf{x}=\mathbf{x}_e \\ \mathbf{u}=\mathbf{u}_e}} \tag{4}$$

For simplicity, the perturbation notation will be dropped in the following sections. That is, referring to the perturbed variables $\delta\mathbf{x}$ and $\delta\mathbf{u}$ by their regular characters $\mathbf{x}$ and $\mathbf{u}$, the linearized state space form of the helicopter dynamic model about a trim point is given by:

$$\dot{\mathbf{x}} = \mathbf{A}\mathbf{x} + \mathbf{B}\mathbf{u} \tag{5}$$

For a helicopter, there are in general four control inputs that can be used by a pilot to cope with six degrees of freedom. These are the main rotor collective θ_0, longitudinal cyclic θ_{1s}, lateral cyclic θ_{1c} and tail rotor collective θ_{0T} or their corresponding stick inputs δ_{col}, δ_{lon}, $\delta_{lat}$and δ_{ped}, as shown in Fig.1. They are collected in the input vector $\mathbf{u}$. The measured outputs are a "standard" set of suitable variables that have physical significance, such as: airspeed, linear accelerations, angular information (rates and attitudes) *etc* (see e.g. [5]). They are either the state variables or can be approximated as known linear combinations of the states and inputs. Thus the measured output vector can be written as:

$$\mathbf{y} = \mathbf{C}\mathbf{x} + \mathbf{D}\mathbf{u} + \mathbf{v} \tag{6}$$

where $\mathbf{v}$ is the measurement noise vector, and matrices $\mathbf{C}$ and $\mathbf{D}$ can usually be derived from $\mathbf{A}$ and $\mathbf{B}$ with the help of the knowledge of the sensor locations.

System identification strategy

As can be seen, the linearized helicopter dynamic model about a trim condition is a continuous-time LTI state-space form as shown in (5). The aim of modelling is to determine the stability and control matrices $\mathbf{A}$ and $\mathbf{B}$ in (5) using the available measurements defined by (6) and the input $\mathbf{u}$. For most practical applications, the measurements are usually sampled-data (i.e. discrete), and so the system identification algorithm will then be implemented in the discrete-time domain. Suppose that the input is constant over the sampling interval T, the sampling/discrete version of the model (5)$\sim$(6) is then given by (see e.g. [6]):

$$\begin{aligned} \mathbf{x}_{k+1} &= \mathbf{\Phi}\mathbf{x}_k + \mathbf{G}\mathbf{u}_k + \mathbf{w}_k & (7) \\ \mathbf{y}_k &= \mathbf{C}\mathbf{x}_k + \mathbf{D}\mathbf{u}_k + \mathbf{v}_k & (8) \end{aligned}$$

where $\mathbf{x}_k \in \Re^n$, $\mathbf{u}_k \in \Re^m$, $\mathbf{y}_k \in \Re^l$, $\mathbf{\Phi} = e^{\mathbf{A}T}$ and $\mathbf{G} = \int_0^T e^{\mathbf{A}\tau}\mathbf{B}d\tau$; $\mathbf{w}_k$ and $\mathbf{v}_k$ are zero-mean white Gaussian sequences of appropriate strength and are independent of the input $\mathbf{u}_k$. The additional term $\mathbf{w}_k$ is added in the state equation (7) as process noise to represent possible atmospheric and other disturbances or the modelling errors due to approximations. Helicopter dynamic model identification then amounts to the determination of matrices $\mathbf{\Phi}$, $\mathbf{G}$ (thus $\mathbf{A}$, $\mathbf{B}$), $\mathbf{C}$ and $\mathbf{D}$ using the measurement sequences $\mathcal{Z} = \{\mathbf{u}_k, \mathbf{y}_k\}_{k=1}^{j}$.

Conventionally, the identification of the above helicopter dynamic model is formulated as a parameter estimation problem. It is essentially a "grey-box" modelling approach, in which a particular model structure and parameterization is prespecified from physical considerations. Model identification then amounts to the estimation of the parameters with which the model is parameterized using either time-domain or frequency-domain methods (see e.g. [5] [1] [2] [3]). Though the physically-relevant model can directly be identified in this way, there are a number of difficulties associated with the application of such a parameter estimation-based method in the identification of a state-space helicopter dynamic model. The first such difficulty lies in the determination of an identifiable model structure or parametrization with respect to the measurements available. This is not a trivial problem, in fact, there is no general method to determine the identifiability of the parameters in a state-space model for the given measurements (except for some state space models of "canonical" forms). The second difficulty stems from the large number of the unknown model parameters resulting from model extension; this may render the parameter estimation-based approach for helicopter modelling impractical. The third difficulty comes from the sensitivity of the conventional nonlinear optimization-based parameter estimation method to the initial values. However, if a "black-box" model structure is assumed or only an input/output relation is of interest, we can then just estimate any matrices $\mathbf{\Phi}$, $\mathbf{G}$ (thus $\mathbf{A}$, $\mathbf{B}$), $\mathbf{C}$ and $\mathbf{D}$ that give a good description of the input-output characteristics of the system such as its frequency response, or realization-independent features such as its poles/eigenvalues. In such cases, the subspace-based system identification method (see e.g. [7], [8], [9], [10]) provides an attractive alternative.

Subspace identification is the name for a general class of relatively new system identification methods; it is essentially a kind of "black-box" modelling technique where the system model is identified without trying to model the internal physical mechanism. The past decade has witnessed significant progress in this field, as can be seen from a large number of survey papers (see e.g. [8], [10]), special issues of journals (see e.g. [11], [12], [13]) and the book by Van Overschee and De Moor [9]. Among the main advantages of such a method, we mention numerical robustness and efficiency, the ability to deal with MIMO problems in a straightforward way and its ease of use due to its simplicity with only a few design parameters that need to be chosen by the user. The method simplifies the identification step and is particularly attractive for high-order MIMO state-space model identification. In the rest of this section, some background on subspace-based identification methods (with particular reference to the MOESP class of algorithm [7]) is presented.

Preliminaries

By repeated substitution of (7) and (8), it is not difficult to obtain the following structured input-output equation:

$$\mathbf{Y}_{k,s,N} = \mathbf{\Gamma}_s \mathbf{X}_{k,N} + \mathbf{H}_s \mathbf{U}_{k,s,N} + \mathbf{E}_s \mathbf{W}_{k,s,N} + \mathbf{V}_{k,s,N} \tag{9}$$

where

$$\mathbf{Y}_{k,s,N} = \begin{bmatrix} \mathbf{y}_k & \mathbf{y}_{k+1} & \cdots & \mathbf{y}_{k+N-1} \\ \mathbf{y}_{k+1} & \mathbf{y}_{k+2} & \cdots & \mathbf{y}_{k+N} \\ \vdots & \vdots & \ddots & \vdots \\ \mathbf{y}_{k+s-1} & \mathbf{y}_{k+s} & \cdots & \mathbf{y}_{k+s+N-2} \end{bmatrix}_{sl \times N} \tag{10}$$

$$\mathbf{H}_s = \begin{bmatrix} \mathbf{D} & \mathbf{0} & \mathbf{0} & \cdots & \mathbf{0} \\ \mathbf{CG} & \mathbf{D} & \mathbf{0} & \cdots & \mathbf{0} \\ \mathbf{C\Phi G} & \mathbf{CG} & \mathbf{D} & \cdots & \mathbf{0} \\ \vdots & \vdots & \vdots & \ddots & \vdots \\ \mathbf{C\Phi}^{s-2}\mathbf{G} & \mathbf{C\Phi}^{s-3}\mathbf{G} & \mathbf{C\Phi}^{s-4}\mathbf{G} & \cdots & \mathbf{D} \end{bmatrix}_{sl \times sm} \tag{11}$$

$\mathbf{U}_{k,s,N}$, $\mathbf{W}_{k,s,N}$ and $\mathbf{V}_{k,s,N}$ are constructed in a manner similar to $\mathbf{Y}_{k,s,N}$ and $\mathbf{E}_s$ similar to $\mathbf{H}_s$ (see e.g. [7] for details). $\mathbf{\Gamma}_s$ is the extended observability matrix for the system to be identified and $\mathbf{X}_{k,N}$ is formed by consecutive state vectors:

$$\mathbf{\Gamma}_s = \begin{bmatrix} \mathbf{C}^T & (\mathbf{C\Phi})^T & \cdots & (\mathbf{C\Phi}^{s-1})^T \end{bmatrix}^T \tag{12}$$

$$\mathbf{X}_{k,N} = \begin{bmatrix} \mathbf{x}_k & \mathbf{x}_{k+1} & \cdots & \mathbf{x}_{k+N-1} \end{bmatrix}_{n \times N} \tag{13}$$

The indices (k, s, N) of the data Hankel matrices $\mathbf{Y}_{k,s,N}$ and $\mathbf{U}_{k,s,N}$ determine their size and what part of the I/O sequences is stored in them. The structured input-output equation (9) is the starting point for subspace-based methods, and all subspace-based algorithms performing state-space model identification are derived from it. From (9), it can be observed that the output block Hankel matrix $\mathbf{Y}_{k,s,N}$ depends in a linear way on the input block Hankel matrix $\mathbf{U}_{k,s,N}$ and the state sequence $\mathbf{X}_{k,N}$. The key to subspace identification is to try to recover the term $\mathbf{\Gamma}_s\mathbf{X}_{k,N}$ in (9) as either the knowledge of $\mathbf{\Gamma}_s$ or $\mathbf{X}_{k,N}$ enables the state-space model matrices in (7) and (8) to be determined. Furthermore, $\mathbf{\Gamma}_s\mathbf{X}_{k,N}$ is a rank deficient term (of rank n, i.e. the system order) which means that once $\mathbf{\Gamma}_s\mathbf{X}_{k,N}$ is obtained, $\mathbf{\Gamma}_s$ and $\mathbf{X}_{k,N}$ can be found simply from an SVD. The model matrices $\mathbf{\Phi}$, $\mathbf{G}$, $\mathbf{C}$ and $\mathbf{D}$ can then be determined (up to a similarity transformation) with the known $\mathbf{\Gamma}_s$ or $\mathbf{X}_{k,N}$.

As a black-box model structure is assumed in the subspace-based method, i.e. the parameterization of the model is not specified before identification, the identified matrices $\mathbf{\Phi}$, $\mathbf{G}$, $\mathbf{C}$ and $\mathbf{D}$ will not be the same as those in the original physically-relevant model. Suppose that the original system is described by (7) and (8) with quadruple $[\bar{\mathbf{\Phi}}, \bar{\mathbf{G}}, \bar{\mathbf{C}}, \bar{\mathbf{D}}]$ and a physically relevant state vector $\bar{\mathbf{x}}$, we then have:

$$\mathbf{\Phi} = \mathbf{T}^{-1}\bar{\mathbf{\Phi}}\mathbf{T} \quad \mathbf{G} = \mathbf{T}^{-1}\bar{\mathbf{G}} \quad \mathbf{C} = \bar{\mathbf{C}}\mathbf{T} \quad \mathbf{D} = \bar{\mathbf{D}} \tag{14}$$

where $\mathbf{T}$ is an invertible matrix (similarity transformation). This corresponds to the change of basis $\mathbf{x}_k = \mathbf{T}^{-1}\bar{\mathbf{x}}_k$ in the state space. It is easy to show that quadruples $[\mathbf{\Phi}, \mathbf{G}, \mathbf{C}, \mathbf{D}]$ and $[\bar{\mathbf{\Phi}}, \bar{\mathbf{G}}, \bar{\mathbf{C}}, \bar{\mathbf{D}}]$ describe the same input-output relationship based on which a controller can be designed.

Since the appearance of subspace system identification in the literature, different subspace algorithms have been derived and used for solving practical problems. A typical algorithm contains two steps: 1.) estimation of the extended observability matrix (12) or the states (13) from the Hankel matrices constructed by the input-output data; and 2.) calculation of state-space matrices from either this extended observability matrix or the estimated states. The MOESP subspace identification algorithm that implements these two steps will be described next.

MOESP type subspace-based state-space model identification

The MOESP (which stands for Multivariable Output-Error State sPace) identification scheme described here was originally proposed in [7] and addresses the problem of identification of the deterministic part of a MIMO state-space model given by (7) and (8). This scheme is chosen because it can be straightforwardly adapted to processing concatenated data sets from multiple tests. This is very helpful for helicopter dynamic modelling for two reasons. Firstly, a helicopter is a MIMO system; as mentioned before, there are four control inputs for a pilot to cope with 6 DoF. A pilot may apply each input in turn during flight tests, and thus we will have a number of data sets with each containing the response generated with mainly one control input. Secondly, the length of a single data run is usually limited due to helicopter instabilities. As a result, a data set may only contain a short period of oscillatory modes which have long time constants, e.g. the phugoid mode. In these cases, we will have to process the multiple or concatenated data sets and it is required that the identification algorithm should be able to identify a single model using such data sets.

To identify a MIMO state space model of (7) and (8) with the MOESP identification algorithm, the I/O equation (9) is split into two parts, a "past" one denoted by subscript p and a "future" one denoted by subscript f:

$$\begin{aligned} \mathbf{Y}_p &= \mathbf{\Gamma}_s\mathbf{X}_p + \mathbf{H}_s\mathbf{U}_p + \mathbf{E}_s\mathbf{W}_p + \mathbf{V}_p && (15) \\ \mathbf{Y}_f &= \mathbf{\Gamma}_s\mathbf{X}_f + \mathbf{H}_s\mathbf{U}_f + \mathbf{E}_s\mathbf{W}_f + \mathbf{V}_f && (16) \end{aligned}$$

where the "past" data Hankel matrices are $\mathbf{Y}_p = \mathbf{Y}_{1,s,N}$ and $\mathbf{U}_p = \mathbf{U}_{1,s,N}$ as defined in (10) with $k = 1$; the "future" data Hankel matrices are $\mathbf{Y}_f = \mathbf{Y}_{s+1,s,N}$ and $\mathbf{U}_f = \mathbf{U}_{s+1,s,N}$ as defined in (10) with $k = s + 1$; $\mathbf{W}_p$, $\mathbf{W}_f$ and $\mathbf{V}_p$, $\mathbf{V}_f$ are noise Hankel matrices formed from the noise sequences $\mathbf{w}_k$ and $\mathbf{v}_k$ in a manner similar to $\mathbf{Y}_p$, $\mathbf{Y}_f$, and $\mathbf{X}_p$, $\mathbf{X}_f$ are defined as in (13) with $k = 1$ and $k = s + 1$ respectively.

The MOESP subspace identification scheme described here is based on the use of both the past input and past output as instrumental variables to remove the effect of noise. The overall algorithm can be summarized as follows (see [7] for details):

Step 1 Perform RQ decomposition of the following compound matrix constructed by the "past" and "future" data Hankel matrices defined in (15) and (16):

$$\begin{bmatrix} \mathbf{U}_f \\ \mathbf{U}_p \\ \mathbf{Y}_p \\ \mathbf{Y}_f \end{bmatrix} = \begin{bmatrix} \mathbf{R}_{11} & \mathbf{0} & \mathbf{0} & \mathbf{0} \\ \mathbf{R}_{21} & \mathbf{R}_{22} & \mathbf{0} & \mathbf{0} \\ \mathbf{R}_{31} & \mathbf{R}_{32} & \mathbf{R}_{33} & \mathbf{0} \\ \mathbf{R}_{41} & \mathbf{R}_{42} & \mathbf{R}_{43} & \mathbf{R}_{44} \end{bmatrix} \begin{bmatrix} \mathbf{Q}_1^{(ms,N)} \\ \mathbf{Q}_2^{(ms,N)} \\ \mathbf{Q}_3^{(ls,N)} \\ \mathbf{Q}_4^{(ls,N)} \end{bmatrix} \tag{17}$$

Step 2 Compute the singular value decomposition (SVD) of the compound matrix $[\mathbf{R}_{42} \;\; \mathbf{R}_{43}]$ as follows:

$$\left[\mathbf{R}_{42} \;\; \mathbf{R}_{43}\right] = ls \begin{array}{c} \begin{matrix} n & ls\text{–}n \end{matrix} \\ \left(\mathbf{U}_n \;\; \mathbf{U}_n^{\perp}\right) \end{array} \underbrace{\begin{array}{c} \begin{matrix} n & ls\text{–}n & ms \end{matrix} \\ \begin{pmatrix} \mathbf{S}_n & \mathbf{0} & \mathbf{0} \\ \mathbf{0} & \mathbf{S}_2 & \mathbf{0} \end{pmatrix} \end{array}}_{\mathbf{S}} \mathbf{V}^T \tag{18}$$

where n is the actual order of the system model to be identified and $\mathbf{U}_n^{\perp}$ stands for the orthogonal complement of $\mathbf{U}_n$ (i.e. $(\mathbf{U}_n^{\perp})^T\mathbf{U}_n = \mathbf{0}$). $\mathbf{S}$ in (18) is a $ls \times (ms+ls)$ matrix with the singular values of the compound matrix $[\mathbf{R}_{42}\ \ \mathbf{R}_{43}]$ along the diagonal in decreasing order and zeros elsewhere. It can be shown (see [7]) that the column space of the matrix $\mathbf{U}_n$ is a consistent estimate of that of $\mathbf{\Gamma}_s$.

If the model order n is also unknown, it can be determined by inspection of the singular values in matrix $\mathbf{S}$ of (18). In the ideal case where the measurements are generated by model (7) and (8) of order n without noise contamination (i.e. $\mathbf{w}_k = \mathbf{0}$, $\mathbf{v}_k = \mathbf{0}$), the compound matrix will have exactly rank n and only the first n singular values will be non-zero (i.e. $\mathbf{S}_2 = \mathbf{0}$). In practice, the $\mathbf{S}$ matrix in (18) will typically have all its singular values non-zero due to the noise. The first n will be supported by $\mathbf{\Gamma}_s$, while the remaining ones will stem from the noise. If the noise is small, one should expect that the latter are significantly smaller than the former. Therefore, the singular values obtained by the SVD specified by (18) provide users with the information for the determination of the order of the underlying system model.

Step 3 By making use of the shift invariance property of $\mathbf{\Gamma}_s$, the matrices $\mathbf{\Phi}$ and $\mathbf{C}$ of state space model (7) and (8) can be determined as follows:

$$\mathbf{C} = \mathbf{U}_n(1:l,:) \tag{19}$$
$$\mathbf{\Phi} = \mathbf{U}_n(1:l(s-1),:)^{+}\mathbf{U}_n(l+1:ls,:) \tag{20}$$

In these two equations, the standard Matlab notation to select a subpart of a matrix is adopted and $(\cdot)^{+}$ denotes the pseudo-inverse of a matrix.

Step 4 It was shown in (e.g. [7],[14]) that the matrices $\mathbf{G}$ and $\mathbf{D}$ in (7) and (8) can be determined by solving a least squares problem derived from I/O equations (15) and (16) with the help of the RQ decomposition (17) and the estimated $\mathbf{\Phi}$ and $\mathbf{C}$ in the last step. However, the simulation studies have shown that the estimates obtained in this way may become sensitive to the noise. In an attempt to overcome the problem, an alternative method is presented here, in which the estimation of the elements in $\mathbf{B}$ and $\mathbf{D}$ and initial state $\mathbf{x}_0$ as well is formulated as a standard linear regression problem.

The state-space model (7) can be rewritten as:

$$\mathbf{x}_k = \mathbf{\Phi}\mathbf{x}_{k-1} + (\mathbf{I}_n \otimes \mathbf{u}_{k-1}^T)vec(\mathbf{G}) + \mathbf{w}_{k-1} \tag{21}$$

where $\otimes$ denotes the Kronecker product and $vec(\mathbf{G})$ is vectorized $\mathbf{G}$ matrix along its rows. The output measurement defined by (8) can then be represented as:

$$\begin{aligned}
\mathbf{y}_k &= \mathbf{C\Phi}\mathbf{x}_{k-1} + \mathbf{C}(\mathbf{I}_n \otimes \mathbf{u}_{k-1}^T)vec(\mathbf{G}) \\
&\quad +(\mathbf{I}_l \otimes \mathbf{u}_k^T)vec(\mathbf{D}) + \mathbf{C}\mathbf{w}_{k-1} + \mathbf{v}_k \\
&= \mathbf{C\Phi}^2\mathbf{x}_{k-2} + \\
&\quad \mathbf{C}[\mathbf{\Phi}(\mathbf{I}_n \otimes \mathbf{u}_{k-2}^T)+(\mathbf{I}_n \otimes \mathbf{u}_{k-1}^T)]vec(\mathbf{G}) + \\
&\quad (\mathbf{I}_l \otimes \mathbf{u}_k^T)vec(\mathbf{D}) + \mathbf{C}[\mathbf{\Phi}\mathbf{w}_{k-2} + \mathbf{w}_{k-1}]+\mathbf{v}_k \\
&\ \ \vdots \\
&= \mathbf{C\Phi}^k\mathbf{x}_0 + \sum_{j=0}^{k-1}\mathbf{C\Phi}^j(\mathbf{I}_n \otimes \mathbf{u}_{k-1-j}^T)vec(\mathbf{G}) \\
&\quad +(\mathbf{I}_l \otimes \mathbf{u}_k^T)vec(\mathbf{D}) + \sum_{j=0}^{k-1}\mathbf{C\Phi}^j\mathbf{w}_{k-1-j} + \mathbf{v}_k
\end{aligned} \tag{22}$$

For the given and fixed $\mathbf{\Phi}$ and $\mathbf{C}$, equation (22) is of the standard linear regression form in terms of $vec(\mathbf{G})$, $vec(\mathbf{D})$ and initial state $\mathbf{x}_0$ and therefore, once $\mathbf{\Phi}$ and $\mathbf{C}$ are determined in step 3, matrices $\mathbf{G}$, $\mathbf{D}$ and initial state $\mathbf{x}_0$ can then be estimated by solving the above linear regression problem using LS.

Remarks

The structured "past" and "future" I/O equations (15) and (16) hold for arbitrary initial conditions, therefore non-zero initial states have no effect at all on the calculations of the quadruples $[\mathbf{\Phi}, \mathbf{G}, \mathbf{C}, \mathbf{D}]$. As such, concatenating different data sets for identification introduces no additional problems. This can be illustrated for two different data sets $\mathcal{Z}^1 = \{\mathbf{u}_k^1, \mathbf{y}_k^1\}_{k=1}^{N_1}$ and $\mathcal{Z}^2 = \{\mathbf{u}_k^2, \mathbf{y}_k^2\}_{k=1}^{N_2}$. The structured "past" and "future" I/O equations for these two data sets are as follows:

$$\mathbf{Y}_p^1 = \mathbf{\Gamma}_s\mathbf{X}_p^1 + \mathbf{H}_s\mathbf{U}_p^1 + \mathbf{E}_s\mathbf{W}_p^1 + \mathbf{V}_p^1 \tag{23}$$
$$\mathbf{Y}_f^1 = \mathbf{\Gamma}_s\mathbf{X}_f^1 + \mathbf{H}_s\mathbf{U}_f^1 + \mathbf{E}_s\mathbf{W}_f^1 + \mathbf{V}_f^1 \tag{24}$$
$$\mathbf{Y}_p^2 = \mathbf{\Gamma}_s\mathbf{X}_p^2 + \mathbf{H}_s\mathbf{U}_p^2 + \mathbf{E}_s\mathbf{W}_p^2 + \mathbf{V}_p^2 \tag{25}$$
$$\mathbf{Y}_f^2 = \mathbf{\Gamma}_s\mathbf{X}_f^2 + \mathbf{H}_s\mathbf{U}_f^2 + \mathbf{E}_s\mathbf{W}_f^2 + \mathbf{V}_f^2 \tag{26}$$

where $\mathbf{Y}_p^1 = \mathbf{Y}_{1,s,N_1-2s+1}$, $\mathbf{U}_p^1 = \mathbf{U}_{1,s,N_1-2s+1}$, $\mathbf{Y}_f^1 = \mathbf{Y}_{s+1,s,N_1-2s+1}$ and $\mathbf{U}_f^1 = \mathbf{U}_{s+1,s,N_1-2s+1}$ are constructed as in (10) with the data from $\mathcal{Z}^1$; and $\mathbf{Y}_p^2$, $\mathbf{U}_p^2$, $\mathbf{Y}_f^2$ and $\mathbf{U}_f^2$ are constructed in a similar way with the data from $\mathcal{Z}^2$. The two "past" data equations (23) and (25) and the two "future" data equations (24) and (26) can readily be combined into the following compact form respectively:

$$\begin{aligned}\left[\mathbf{Y}_p^1|\mathbf{Y}_p^2\right] &= \mathbf{\Gamma}_s\left[\mathbf{X}_p^1|\mathbf{X}_p^2\right] + \mathbf{H}_s\left[\mathbf{U}_p^1|\mathbf{U}_p^2\right] \\ &\quad + \mathbf{E}_s\left[\mathbf{W}_p^1|\mathbf{W}_p^2\right] + \left[\mathbf{V}_p^1|\mathbf{V}_p^2\right] \quad (27) \\ \left[\mathbf{Y}_f^1|\mathbf{Y}_f^2\right] &= \mathbf{\Gamma}_s\left[\mathbf{X}_f^1|\mathbf{X}_f^2\right] + \mathbf{H}_s\left[\mathbf{U}_f^1|\mathbf{U}_f^2\right] \\ &\quad + \mathbf{E}_s\left[\mathbf{W}_f^1|\mathbf{W}_f^2\right] + \left[\mathbf{V}_f^1|\mathbf{V}_f^2\right] \quad (28)\end{aligned}$$

These combined "past" and "future" data equations are of the same structure as the original "past" and "future" data equations (15) and (16) apart from the fact that the combined or concatenated I/O data matrices $[\mathbf{Y}_p^1|\mathbf{Y}_p^2]$, $[\mathbf{Y}_f^1|\mathbf{Y}_f^2]$, $[\mathbf{U}_p^1|\mathbf{U}_p^2]$ and $[\mathbf{U}_f^1|\mathbf{U}_f^2]$ are no longer Hankel. However, as the Hankel property is not exploited in the derivation of the MOESP algorithm, the main body of the algorithm described above can still be used when starting with an RQ decomposition of the following data matrix:

$$\left[\begin{array}{c|c}\mathbf{U}_f^1 & \mathbf{U}_f^2 \\ \mathbf{U}_p^1 & \mathbf{U}_p^2 \\ \mathbf{Y}_p^1 & \mathbf{Y}_p^2 \\ \mathbf{Y}_f^1 & \mathbf{Y}_f^2\end{array}\right] \quad (29)$$

As such, the MOESP algorithm can be readily modified for helicopter dynamic model identification using concatenation of data sets from multiple tests.

As can be seen, the basic computational steps in the MOESP algorithm described are amazingly simple, being based on the QR decomposition and SVD for which numerically efficient and stable algorithms and software are available. An additional advantage of the aforementioned algorithm is that there is essentially only one design parameter which needs to be specified by the user, i.e. the dimensioning parameter s of the data Hankel matrix. The basic requirement for the parameter is $s > n$, which indicates that the selection of this parameter only requires a rough estimate of the underlying system order.

Applicability studies via simulations

To study the applicability and to illustrate the operation of the identification scheme described in the last section for helicopter dynamic modelling, the problem of identifying an extended dynamic model for a small-scale unmanned rotorcraft is considered in this section. The data is generated from a 13th order unmanned rotorcraft (Yamaha R-50) model taken from [3]. The model describes the dynamics of the perturbed motion about the hover condition of the vehicle and is extended to include the additional dynamics from the rotor and control augmentation such as the active yaw damping system and the stabilizer bar. The model is of the form of (5) where the 13-dimensional state vector is defined as (see [3] for details):

$$\mathbf{x} = \left[\, u\ v\ p\ q\ \phi\ \theta\ a\ b\ w\ r\ r_{fb}\ c\ d \,\right]^T \quad (30)$$

where u, v, w and p, q, r are the translational and rotational velocities of the 6 DoF fuselage; ϕ and θ are the roll and pitch angle of the fuselage; a and b denote the longitudinal and lateral rotor flapping angles; c and d denote the longitudinal and lateral stabilizer bar flapping angles and r_{fb} is a state variable for the active yaw damping dynamics. The input vector includes the four stick inputs as shown in Fig. 1, i.e. $\mathbf{u} = [\delta_{lat}\ \delta_{lon}\ \delta_{ped}\ \delta_{col}]^T$. The true system eigenvalues are calculated with the parameter values provided in [3] and are listed in the first column of Table 1.

The measured outputs available for identification are the rigid-body fuselage states including the translational velocities u, v, w and rotational rates p, q, r; roll and pitch angles ϕ, θ and the accelerations $\dot{u}$, $\dot{v}$, $\dot{w}$ as well. Therefore the measurement vector is defined as:

$$\mathbf{y} = \left[\, u\ v\ p\ q\ \phi\ \theta\ w\ r\ \dot{u}\ \dot{v}\ \dot{w} \,\right]^T \quad (31)$$

In the present simulation studies, a doublet signal is applied to each one of the four control channels in turn and the data are then concatenated for model identification using the MOESP scheme.

The design parameter of the MOESP identification scheme is selected as $s = 20$ in the following simulation studies. To demonstrate the capabilities of the MOESP scheme in handling concatenated data sets, the data sets are processed one after the other. The singular values obtained from equation (18) in the MOESP identification scheme using different concatenations of the measurements specified by (31) are plotted in Fig.2 for the determination of model order, where a "+" indicates a singular value obtained by processing the data set due to δ_{lat} only; a "$*$" indicates a singular value obtained by processing data sets due to δ_{lat} and δ_{lon}; a "o" indicates a singular value obtained by processing data sets due to δ_{lat}, δ_{lon} and δ_{ped}; a "$\times$" indicates a singular value obtained by processing all four data sets.

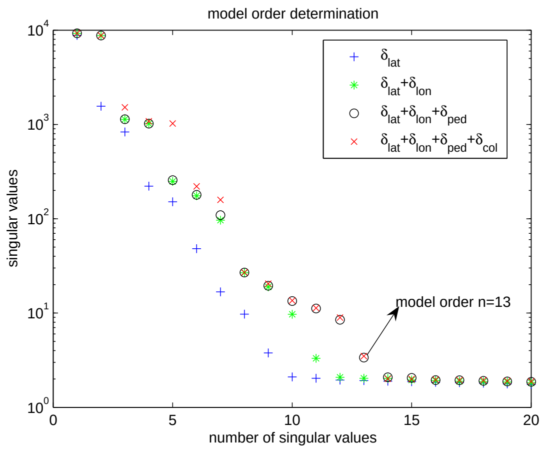

Figure 2: Singular values computed by the MOESP identification scheme using different concatenated data sets

Although all singular values are non-zero due to noise as can be seen from Fig.2, the following observations can be made:

1. There is no clear gap between the 13th and 14th singular values after processing the data set due to δ_{lat} only, as shown by the singular values specified by "+" in Fig.2. The model order would probably be determined as 9 from this data set alone as a clear gap can be observed between the 9th and 10th singular values (as specified by "+" in Fig.2).
2. For the same reason as described above, the model order would be set to 11 from the singular values obtained by processing data sets due to δ_{lat} and δ_{lon} as specified by "$*$" in Fig.2.
3. The correct model order can be determined after processing the data sets due to δ_{lat}, δ_{lon} and δ_{ped} or all four data sets because a clear gap can be seen between the 13th and 14th singular values specified by "o" or "$\times$" in Fig.2. It also can be observed that the singular values due to noise (i.e. from 14th singular value onwards) have approximately the same magnitudes.

Based on the above observations, we may conclude that the concatenation of the data sets due to different control inputs is necessary for identification of a coupled full state-space helicopter model.

Once the model order is determined, the system matrices can be computed as described in last section. The MOESP identification method produces a discrete-time "similarity" state-space model that describes the same input-output relationship as the original system model. To facilitate comparison, the identified discrete-time model is transformed to a continuous-time model and the eigenvalues computed from this continuous-time model are compared with the nominal ones from which the data was generated. The eigenvalue estimates computed using all four data sets are listed in the second column of Table 1. A good match between the estimated eigenvalues and the nominal ones can be observed. Fig.3 shows a comparison between the frequency responses computed from the identified model and those computed from the true model that generates the data. It can be seen, from these figures, that the predicted frequency responses from the identified model match quite well with the true

Table 1: Comparison of identified eigenvalues with the true eigenvalues

true eigenvalues	identified eigenvalues
$\lambda_i(\mathbf{A}) = \begin{cases} 0.306 \pm j0.094 \\ -0.401 \pm j0.086 \\ -0.608 \\ -1.698 \pm j8.189 \\ -6.198 \pm j8.197 \\ -2.661 \pm j11.557 \\ -20.313 \pm j4.743 \end{cases}$	$\lambda_i(\hat{\mathbf{A}}) = \begin{cases} 0.306 \pm j0.094 \\ -0.400 \pm j0.084 \\ -0.608 \\ -1.595 \pm j8.146 \\ -6.190 \pm j8.201 \\ -2.642 \pm j11.540 \\ -20.943 \pm j4.955 \end{cases}$

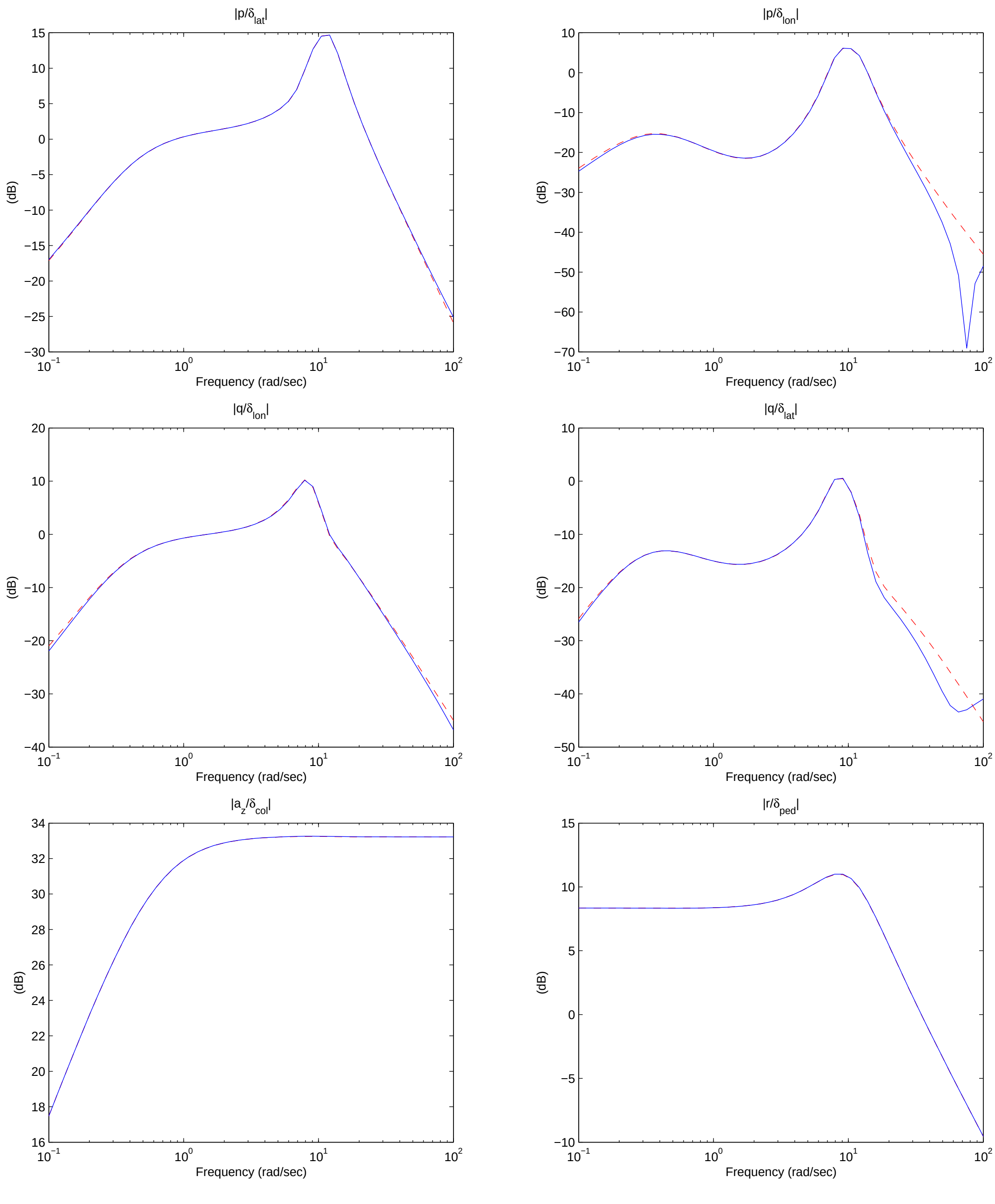

Figure 3: Comparison between the frequency responses derived from the identified model (solid-line) and those computed from true model(dashed-line)

ones computed with the model that generates the data in most cases, the noticeable mismatch can only be observed at the high frequency parts of the off-axis angular responses (p to δ_{lon} and q to δ_{lat}).

Results from real flight test data

As part of the DARP research project "Towards Robust and Cost Effective Approaches to Rotorcraft Design", the MOESP identification scheme was applied to the identification of an extended dynamic model in cruise condition for the EH101 helicopter using real flight test data from Westland Helicopters Ltd (WHL).

The linearised EH101 helicopter dynamic model is assumed to be of the state-space form of (5). The available measured inputs to the system are the main rotor collective blade angle θ_0, main rotor pitch blade angle θ_{1s}, main rotor roll blade angle θ_{1c} and tail rotor collective blade angle θ_{0T} as shown in Fig. 1. The measured outputs available for identification include: the perturbed fuselage longitudinal velocity u; the fuselage rotational rates p, q, r; the fuselage roll and pitch attitudes ϕ, θ; and the fuselage lateral and vertical accelerations $\dot{v}$ and $\dot{w}$. Therefore, the measured output vector is defined as:

$$\mathbf{y} = \left[u \; p \; q \; r \; \phi \; \theta \; \dot{v} \; \dot{w} \right]^T \qquad (32)$$

These I/O data are collected with a constant cruise speed around 80 knots. The singular values containing the information on the model order computed by the MOESP scheme are plotted in Fig.4. The results are obtained with the design parameter chosen as $s = 26$.

From prior knowledge, the order of a full helicopter dynamic model must be greater than six. We can therefore specify the model order as $n = 13$ because a clear large gap between the 13th and 14th singular values can be identified in Fig.4. The corresponding eigenvalue estimates are listed below:

$$\lambda_i(\hat{\mathbf{A}}) = \begin{cases} 0.0816 \pm j0.2281 \\ -0.1171 \pm j5.5117 \\ -0.1171 \\ -0.5402 \pm j0.7872 \\ -0.0624 \pm j22.293 \\ -3.2434 \pm j40.302 \\ -0.5700 \pm j44.506 \end{cases} \qquad (33)$$

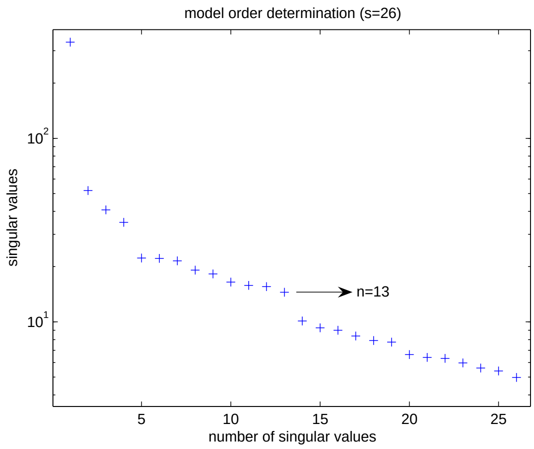

Figure 4: Singular values computed by the MOESP identification scheme using data from EH101 helicopter flight tests

Concluding Remarks

The problem of identifying a state-space helicopter dynamic model using a time-domain system identification technique is studied. The MOESP type of subspace identification method is used. Simulation studies have been carried out to assess the performance of the method and the main results can be summarized as follows:

- The subspace identification method is essentially a "black-box" modelling approach where no prior parameterization of the model to be identified is required. This is very helpful for helicopter dynamic modelling as the determination of an identifiable parameterization for the helicopter dynamic model is far from trivial, especially when only limited measurement channels are available.
- The method is computationally efficient and numerically reliable. This makes it particularly attractive here because the identification of a high order state-space helicopter dynamic model is required.

- The MOESP identification scheme is easy to use (only one simple design parameter needs to be specified by the user) and can deal with the concatenation of the data sets from multiple tests in a straightforward way.

As a "black-box" model structure is assumed, no attempt is made to identify the internal structure of the real system that generates the data in the proposed identification scheme. The method only produces a model that describes the input-output relationship of the original system model. If a particular parametric helicopter model structure or the values of the parameters themselves are of interest, then parameter estimation-based modelling methods (such as e.g. [15],[16]) need to be used. In such cases, a valid identifiable parametric model structure needs to be determined before proceeding to the parameter estimation stage. Subspace-based method as described in this paper can then be used to get some information of the underlying state-space model, such as the possible order of the system, from flight test data.

In the paper, the MOESP identification scheme was also applied to real flight test data from WHL and an extended state-space dynamic model for the cruise condition of an EH101 helicopter was identified. Further work is being carried out to validate the identified model and research is also being performed to develop the practical methods for determining uncertainty in the helicopter dynamic models identified by subspace-based method.

Acknowledgements

The authors wish to thank Westland Helicopters Ltd (WHL) for provision of the flight test data. Funding support from the UK Department of Trade and Industry (DTI) and Ministry of Defence (MoD) under the Rotorcraft Aeromechanics DARP Programme is also gratefully acknowledged.

References

[1] Tischler, M. B., & Cauffman, M. G., (1992) Frequency-Response Method for Rotorcraft System Identification: Flight Application to BO-105 Coupled Rotor/Fuselage Dynamics. *Journal of the American Helicopter Society*, **37**(3), pp3-17.

[2] Fletcher, J. W., (1995) Identification of UH-60 Stability Derivative Models in Hover from Flight Test Data. *Journal of the American Helicopter Society*, **40**(1), pp32-46.

[3] Mettler, B., Tischler, M. B., & Kanade, T., (2002) System Identification Modelling of a Small-Scale Unmanned Rotorcraft for Flight Control Design. *Journal of the American Helicopter Society*,**47**(1), pp50-63.

[4] Padfield, G. D., (1996). *Helicopter Flight Dynamics*. Blackwell Science Ltd, Oxford, UK.

[5] AGARD LS-178 (1991) *AGARD Lecture Series on Rotorcraft system identification.*

[6] Maybeck, P. S. (1982). *Stochastic Models, Estimation, and Control—Volume 2.* Academic Press, 111 Fifth Avenue, New York.

[7] Verhaegen, M., (1994) Identification of the Deterministic Part of MIMO State Space Models Given in Innovations Form from Input-Output Data. *Automatica*, **30**(1), pp61-74.

[8] Viberg, M., (1995) Subspace-based Methods for the Identification of Linear Time-invariant Systems. *Automatica*, **31**(12), pp1835-1852.

[9] Van Overschee, P., & De Moor, B., (1996) *Subspace identification for linear system: Theory, Implementation, Applications*, Kluwer Academic Publishers, Dordrecht.

[10] Favoreel, W., De Moor, B., & Van Overschee, P., (2000) Subspace state space system identification for industrial processes. *Journal of Process Control* **10**(2-3), pp149-155.

[11] Special Issue on Statistical Signal Processing and Control. (1994) *Automatica*, **30**(1)

[12] Special Issue on System Identification. (1995) *Automatica*, **31**(12)

[13] Special Issue on Subspace Methods for System Identification. (1996) *Signal Processing*, **52**(2)

[14] Wang, J. & Qin, S. J. (2002) A new subspace identification approach based on principal component analysis. *Journal of Process Control*, **12**, pp841-855.

[15] Ljung, L. (1999). *System Identification—Theory for the User*. Prentice-Hall, Upper Saddle River, NJ.

[16] Li, P., Goodall, R. M., & Kadirkamanathan, V. (2004). Estimation of parameters in a linear state space model using a Rao-Blackwellised particle filter. *IEE Proceedings-Control Theory and Application*, **151**, No.6, pp727-738.